

Palladium Porphyrin Containing Zirconium Phosphonate Langmuir–Blodgett Films

Christine M. Nixon,[†] Karine Le Claire,[‡] Fabrice Odobel,^{*,‡} Bruno Bujoli,^{*,‡} and Daniel R. Talham^{*,†}

Department of Chemistry, University of Florida, Gainesville, FL 32611-7200, and Laboratoire de Synthèse Organique, Faculté des Sciences et des Techniques, BP 92208, 44322 NANTES Cedex 03

Received September 14, 1998. Revised Manuscript Received January 14, 1999

The substituted tetraphenylporphyrins palladium 5,10,15,20-tetrakis(2',3',5',6'-tetrafluorophenyl-4'-octadecyloxyphosphonic acid)porphyrin (**16**) and palladium 5,10,15-tris(2',6'-dichlorophenyl)-20-(2',3',5',6'-tetrafluorophenyl-4'-octadecyloxyphosphonic acid)porphyrin (**17**) have been studied as Langmuir monolayers and as zirconium phosphonate Langmuir–Blodgett (LB) films. Using a three-step deposition technique, symmetric and alternating zirconium phosphonate bilayers and multilayers were prepared. In these films, the porphyrin constituent resides in the hydrophobic region of the monolayer and the phosphonate substituents bind zirconium ions in the hydrophilic part. Films of the pure porphyrins and of mixtures with octadecylphosphonic acid (OPA) were prepared. Langmuir monolayers were characterized with pressure vs area isotherms and reflectance UV–vis spectroscopy. LB films were studied with transmittance UV–vis and X-ray diffraction. Control over chromophore interaction was achieved by chemical modification of the amphiphiles and by selection of appropriate transfer conditions. For example, reduced aggregation was seen in LB films of the tetraphosphonic acid substituted porphyrin **16** transferred at mean molecular areas (MMA) larger than the area per molecule of the substituted porphyrin. In these films, the porphyrin macrocycles are nonaggregated and oriented parallel to the surface. In contrast, the monophosphonic acid substituted **17** aggregates under all of the deposition conditions studied. The stability of the porphyrin LB films was examined by exposing the films to refluxing chloroform. UV–vis absorbance after immersion in chloroform confirmed conclusions that in films of **17**, many of the chromophores are not tethered to the inorganic network and are easily removed, whereas in films of **16**, all molecules bind to the zirconium phosphonate extended network, making these films very resilient.

Introduction

Organized porphyrin films that mimic biomaterials have long been of interest for applications that include selective gas sensing,¹ photovoltaic devices,^{2,3} electron transfer,^{4–6} and catalysis.^{4,7–9} The Langmuir–Blodgett (LB) technique is a versatile method used to prepare highly ordered films with a layered architecture and is one of many methods employed to form organized porphyrin films.^{10–12} Typically, LB films containing

porphyrin constituents have been studied in which the chromophore itself is the polar headgroup. These porphyrin films have been successfully prepared with either the molecule sufficiently diluted with a film stabilizing amphiphile,^{9,13–15} such as stearic acid, or with long hydrophobic chains attached to the chromophore to stabilize the monolayer on the water surface.^{16,17} However, in nearly all porphyrin-containing LB films, there is significant aggregation of the chromophores which can greatly influence the properties of the porphyrin films.

The aggregation, or chromophore π – π interactions, is often a consequence of the film-forming procedures.

* To whom correspondence should be addressed.

[†] University of Florida.

[‡] Faculté des Sciences et des Techniques.

(1) Arnold, D.; Manno, D.; Micocci, A.; Tepore, A.; Valli, L. *Langmuir* **1997**, *13*, 5951–5956.

(2) Zhang, J.; Wang, D.; Chen, Y.; Li, T.; Mao, H.; Tian, H.; Zhou, Q.; Xu, H. *Thin Solid Films* **1997**, *300*, 208–212.

(3) O'Keefe, G.; Halls, J.; Walsh, C.; Denton, G.; Friend, R.; Anderson, H. *Chem. Phys. Lett.* **1997**, *276*, 78–83.

(4) Groves, J.; Neumann, R. *J. Am. Chem. Soc.* **1989**, *111*, 2900–2909.

(5) Jolliffe, K.; Bell, T.; Ghiggino, K.; Langford, S.; Paddon-Row, M. *Angew. Chem. Int. Ed. Engl.* **1998**, *37*, 916–919.

(6) Ishida, A.; Sakata, Y.; Majima, T. *Chem. Lett.* **1998**, 267–268.

(7) Gilmarten, C.; Lindsay Smith, J. *J. Chem. Soc. Perkin Trans.* **1995**, *2*, 243–251.

(8) Miki, K.; Sato, Y. *Bull. Chem. Soc. Jpn.* **1993**, *66*, 2385–2390.

(9) Abatti, D.; Zanicelli, M. E.; Iamamoto, Y.; Idemori, Y. *Thin Solid Films* **1997**, *310*, 296–302.

(10) Ulman, A. *An Introduction to Ultrathin Organic Films: From Langmuir–Blodgett to Self-Assembly*; Academic Press: Boston, 1991.

(11) Roberts, G. G. *Langmuir–Blodgett Films*; Plenum Press: New York, 1990.

(12) Blodgett, K. B. *J. Am. Chem. Soc.* **1935**, *57*, 1007.

(13) Zhang, Z.; Nakashima, K.; Lal Verma, A.; Yoneyama, M.; Iriyama, K.; Ozaki, Y. *Langmuir* **1998**, *14*, 1177–1182.

(14) Anikin, M.; Tkachenko, N.; Lemmetyinen, H. *Langmuir* **1997**, *13*, 3002–3008.

(15) Honeybourne, C.; Barrell, K. *J. Mater. Chem.* **1996**, *6*, 323–329.

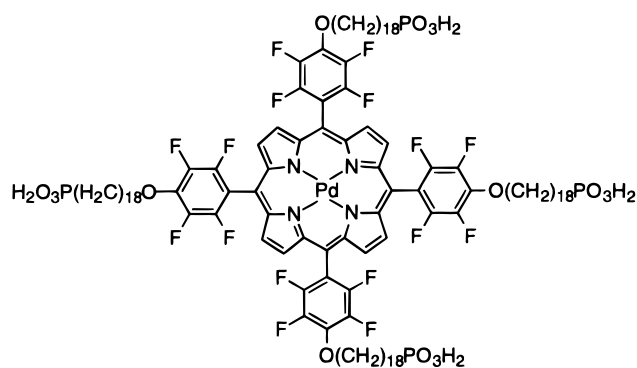
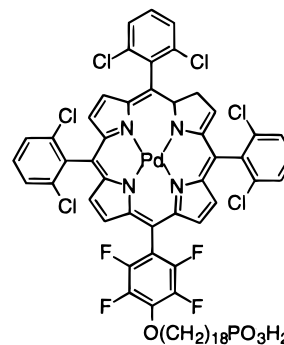
(16) Ruau-del-Teixier, A.; Barraud, A.; Belbeoch, B.; Roulliay, M. *Thin Solid Films* **1983**, *99*, 33–40.

(17) Kroon, J.; Sudholter, E.; Schenning, A.; Nolte, R. *Langmuir* **1995**, *11*, 214–220.

First, compression of the film on the water surface forces the eventual overlap or tilting of the chromophores.^{9,15,17} Also, the decreased affinity of the derivatized chromophores for water tends to force the chromophores to aggregate rather than to spread on the water surface.¹⁸ Understanding the molecular orientation, aggregation, and morphology of porphyrin LB films is critical because each is intimately linked to chromophore behavior. For example, aggregation can significantly reduce or eliminate the efficiency of the porphyrin in catalysis¹⁹ or the ability of the porphyrin to bind probe molecules in a sensor.¹⁸ Therefore, it is desirable to find methods for forming porphyrin LB films with no aggregation.

We have recently developed a new class of LB films that are modeled after solid-state metal phosphonates, which are organic/inorganic layered solids containing inorganic continuous lattice layers separated by layers of the organic phosphonic acid substituent.^{20–30} Metal phosphonate LB films with divalent,^{25,31} trivalent,^{28,29} and tetravalent^{20,21,23,24} metal ions have all been described, and in each case, the inorganic continuous lattice network in the LB film has the same in-plane structure as the complementary solid-state analogues. The inorganic network provides enhanced stability to these films through substantial ionic/covalent lattice energy. In addition, the inorganic network can be chosen to introduce physical phenomenon, such as magnetic order, into the LB film.³¹

Langmuir monolayers and LB films of the derivatized palladium tetraphenyl porphyrin molecules **16** and **17** are described in this paper. Porphyrins **16** and **17** are substituted with four and one octadecylphosphonic acid groups, respectively. These molecules differ from many other porphyrin amphiphiles in that there is a hydrophilic group at the end of the alkyl chain substituent. Most often, the porphyrin group is the hydrophilic part of LB film forming amphiphiles.¹⁶ Molecules **16** and **17** were designed to investigate whether porphyrins can be incorporated into metal phosphonate LB films and to study how the orientation and aggregation of the porphyrin can be controlled in the deposited films.

**16****17**

Palladium polyhalogenated porphyrins were chosen on the basis of the following considerations. First, palladium porphyrins are not demetalated under acidic conditions, and their diamagnetic character makes following the synthesis with NMR spectroscopy possible. Second, manganese and iron polyhalogenated porphyrins are well-known catalysts for the oxidation of hydrocarbons;³² therefore, if palladium is replaced by these metals, the films can be used for catalytic applications. Third, pentafluorophenyl substituents on porphyrins allow straightforward functionalization of this ligand by aromatic nucleophilic displacement with an alcohol. In addition, the ether bonds are more stable toward hydrolysis and less hydrophilic than the ester or amide linkages usually used to tether alkyl chains on porphyrins. High hydrophobicity of the linkage is a requirement because competition with the polar phosphonic acid headgroup should be avoided during the LB film preparation.

In the present study, LB films of **16** and **17** are formed as zirconium phosphonates. The strong tendency of zirconium ions to cross-link the phosphonate groups precludes the normal deposition of organophosphonate monolayers with the metal in the subphase.²³ Therefore, a previously developed three-step deposition procedure was used (Scheme 1).^{23,24} A phosphonic acid monolayer is first transferred on the down stroke onto a hydrophobic substrate to form a "template layer". The substrate is then removed from the trough and placed in a Zr⁴⁺ solution to bind the metal ions. In step three, the zirconated template is placed back in the trough and a phosphonic acid "capping layer" is deposited as the

(18) Song, X.; Miura, M.; Xu, X.; Taylor, K.; Majumder, S.; Hobbs, J.; Cesarano, J.; Shelnut, J. *Langmuir* **1996**, *12*, 2019–2027.

(19) Schenning, A.; Hubert, D.; Feiters, M.; Nolte, R. *Langmuir* **1996**, *12*, 1572–1577.

(20) Byrd, H.; Pike, J. K.; Talham, D. R. *Synth. Met.* **1995**, *71*, 1977–1980.

(21) Byrd, H.; Pike, J. K.; Showalter, M. L.; Whipps, S.; Talham, D. R. In *Interfacial Design and Chemical Sensing*; Mallouk, T. E., Harrison, D. J., Eds.; Series 561 Vol. ACS Symposium; American Chemical Society: Washington, 1994; 49–59.

(22) Byrd, H.; Pike, J. K.; Talham, D. R. *Thin Solid Films* **1994**, *242*, 100–105.

(23) Byrd, H.; Pike, J. K.; Talham, D. R. *Chem. Mater.* **1993**, *5*, 709–715.

(24) Byrd, H.; Whipps, S.; Pike, J. K.; Ma, J.; Nagler, S. E.; Talham, D. R. *J. Am. Chem. Soc.* **1994**, *116*, 295–301.

(25) Byrd, H.; Pike, J. K.; Talham, D. R. *J. Am. Chem. Soc.* **1994**, *116*, 7903–7904.

(26) Seip, C. T.; Byrd, H.; Talham, D. R. *Inorg. Chem.* **1996**, *35*, 3479–3483.

(27) Talham, D. R.; Seip, C. T.; Whipps, S.; Fanucci, G. E.; Petruska, M. A.; Byrd, H. *Comments Inorg. Chem.* **1997**, *19*, 133–151.

(28) Fanucci, G. E.; Seip, C. T.; Petruska, M. A.; Ravaine, S.; Nixon, C. M.; Talham, D. R. *Thin Solid Films* **1998**, *327–329*, 331–335.

(29) Fanucci, G. E.; Talham, D. R. *Langmuir* Submitted for publication.

(30) Petruska, M. A.; Fanucci, G. E.; Talham, D. R. *Chem. Mater.* **1998**, *10*, 177–189.

(31) Seip, C. T.; Granroth, G. E.; Meisel, M. W.; Talham, D. R. *J. Am. Chem. Soc.* **1997**, *119*, 7084–7094.

(32) Montanari, F. *Metalloporphyrins Catalysed Oxidations*; Kluwer Academic Publishers: 1994.

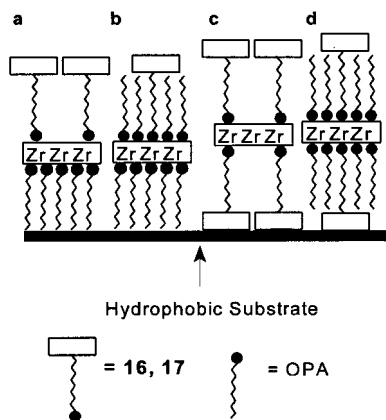
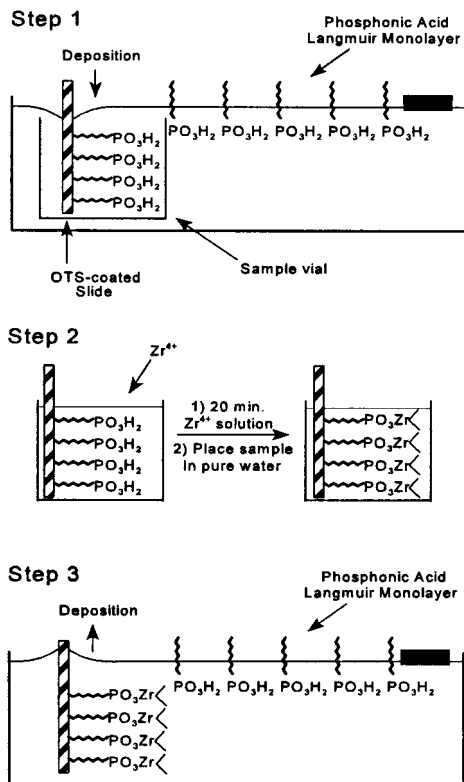


Figure 1. Schematic of the porphyrin containing films formed by the three-step deposition procedure: (a) alternating film where the template layer is OPA and the capping layer is pure porphyrin (OPA/Zr/porphyrin), (b) alternating film where the template layer is OPA and the capping layer is porphyrin mixed with OPA (OPA/Zr/% porphyrin), (c) symmetric film where both template and capping layers are pure porphyrin (porphyrin/Zr/porphyrin), and (d) symmetric film where both template and capping layers are porphyrin mixed with OPA (porphyrin/Zr/% porphyrin).

Scheme 1. Three-Step Deposition Procedure for the Formation of Zirconium-Phosphonate Bilayers



substrate is withdrawn. Both symmetric (porphyrin/Zr/porphyrin) and alternating (octadecylphosphonic acid (OPA)/Zr/porphyrin) films can be prepared in this way (Figure 1).

Control over aggregation of the porphyrin chromophores is achieved through a combination of molecular design and the careful choice of the conditions for transfer of the films. Aggregation is decreased or eliminated in the films of the tetrasubstituted **16** when transferred at very high mean molecular area MMA and

at high subphase pH. Mixtures of this amphiphile with OPA transferred at high temperatures (40 °C) and high MMA showed a similar decrease in interchromophore interaction. The four long-chain phosphonic acid substituents significantly aid the spreading of monomeric porphyrin species, and the strength of the zirconium phosphonate interaction ensures their isolation in the transferred films. In similar studies of the monosubstituted **17**, aggregation was observed under all of the transfer conditions explored, indicating that none of the deposition procedures overcome the tendency of the molecules to aggregate.

Experimental Section

Synthesis. Materials. The following chemicals have been prepared according to literature procedures: 9-bromo-1-nonanol,³³ 5,10,15-tris(2,6-dichlorophenyl)-20-(pentafluorophenyl)porphyrin,³⁴ and 5,10,15,20-tetrakis(pentafluorophenyl)porphyrin.³⁵ Solvents were dried by standard methods before use. Column chromatography was performed on Kieselgel 60, 230–400 mesh silica gel (Merck 9385).

Instrumentation. All NMR spectra were recorded on a Bruker AM 200. Reported proton chemical shifts are referenced to the nondeuterated solvent signal (CD₃CN, 1.94 ppm; CD₃OD, 4.5 ppm; CDCl₃, 7.26 ppm). ³¹P spectra were recorded fully decoupled, and the chemical shifts are referenced to H₃-PO₄ as an internal standard. ¹⁹F spectra were referenced with respect to FCCL₃ assigned to 0 ppm. FAB-MS analyses were performed in a *m*-nitrobenzyl alcohol matrix (MBA) on a ZAB-HF-FAB (fast atom bombardment) spectrometer, and EI-MS (electronic impact) spectra were recorded on quadrupole HP 5889A spectrometer (70 eV) with results given as follows: *m/z* (intensity of the signal).

1-Tetrahydropyranyloxy-9-bromononane (3). A 5 g portion of 9-bromo-1-nonanol (**2**) (22.4 mmol) was stirred at room temperature under an argon atmosphere with 21.5 mL of dihydropyrene (24.6 mmol) in 50 mL of anhydrous ether in the presence of 20 mg of TsOH (0.1 mmol) for 8 h. The reaction mixture was diluted with CH₂Cl₂, washed with water, and dried over MgSO₄. The crude oil was purified by column chromatography on silica (eluent CH₂Cl₂/hexane 4/6) leading to a colorless oil in 82% yield. ¹H NMR (CDCl₃, ppm): 1.29 (s, br, 12H, CH₂ chain and CH₂ from THP), 1.54 (m, 2H, CH₂-CH₂Br), 1.71 (m, 4H, CH₂ from THP), 1.88 (m, 2H, CH₂CH₂O-THP), 3.39 (m, 4H, CH₂Br and CH₂O from THP), 3.70 (m, 2H, CH₂O-THP), 4.56 (s, br, 1H, OCHO). ¹³C NMR (CDCl₃, ppm): 18.69–31.82 (CH₂), 32.89 (CH₂Br), 61.29 (CH₂O-THP), 66.60 (CH₂O from THP), 97.81 (OCHO). EI MS: *m/z* = 305/307 (4), 85 (100), 69 (29), 57 (28), 56 (33), 55 (29), 41 (32).

1-Tetrahydropyranyloxy-1-undecyne (4). Under an argon atmosphere, a solution of lithium acetylide-ethylenediamine (1.8 g, 19.5 mmol) in dry DMSO (8 mL) was cooled in an ice bath. Compound **3** was added dropwise and the mixture was stirred overnight at room temperature. The resulting mixture was diluted with 150 mL of water and was extracted several times with the mixture CH₂Cl₂/ether 9/1. The organic phase was dried over MgSO₄, and the solvents were rotary evaporated. The viscous liquid was purified on silica column chromatography eluted with the mixture CH₂Cl₂/hexane 2/8 to give 3.32 g of the terminal alkyne **4** in 82% yield. ¹H NMR (CDCl₃, ppm): 1.28–1.83 (m, 20H, CH₂ chain and CH₂ from THP), 1.91 (t, 1H, ⁴J_{H-H} = 2.4 Hz, CH terminal alkyne), 2.15 (dt, 2H, ³J_{H-H} = 6.4 Hz, ⁴J_{H-H} = 2.4 Hz, CH₂ alkyne), 3.42 (m, 2H, CH₂O from THP), 3.78 (m, 2H, CH₂O-THP), 4.55 (s, br, 1H, OCHO). ¹³C NMR (CDCl₃, ppm): 17.37–29.68 (CH₂), 61.23 (CH₂O-THP), 66.61 (CH₂O from THP), 67.08 (CH terminal alkyne), 83.64 (C alkyne), 97.78 (OCHO). EI MS: *m/z*

(33) Kang, S.; Kim, W.-S.; Moon, B.-H. *Synthesis* **1985**, 1161–1162.

(34) Battioni, P.; Redon, A.; Mansuy, D. Private communications.

(35) Lindsey, J.; Wagner, R. J. *Org. Chem.* **1989**, *54*, 828–836.

= 251 (1), 101 (27), 85 (100), 67 (20), 56 (18), 55 (19), 43 (12), 41 (28).

1-Tetrahydropyranyloxy-18-bromo-11-undecyne (5). Under an argon atmosphere, a solution of compound **4** (3.28 g; 13 mmol) in 30 mL of dry THF was cooled to -40°C . To this cold solution, $n\text{BuLi}$ (solution in hexane 1.6 M, 13.7 mmol) was added dropwise with stirring and the mixture was allowed to warm gradually to room temperature while being stirred. After 1 h, the deep red solution was cooled again to -40°C and 10 mL of dry HMPA was added, followed by addition of 15 g of 1,7-dibromoheptane (58 mmol). The solution was allowed to warm to room temperature and stirred overnight. The solvent was removed under vacuum. The crude product was dissolved with CH_2Cl_2 , washed with water, and dried over MgSO_4 , and then the oil was purified by column chromatography on silica gel (eluent $\text{CH}_2\text{Cl}_2/\text{hexane}$ 5/5) to give 4.8 g of **5** as a colorless oil in 86% yield. $^1\text{H NMR}$ (CDCl_3 , ppm): 1.30–1.87 (m, 30H, CH_2 chain and CH_2 from THP), 2.14 (m, 4H, CH_2C alkyne), 3.44 (m, 4H, CH_2Br and CH_2O from THP), 3.79 (m, 2H, CH_2O –THP), 4.57 (s, br, 1H, OCHO). $^{13}\text{C NMR}$ (CDCl_3 , ppm): 17.69–31.76 (CH_2), 32.82 (CH_2Br), 61.29 (CH_2O –THP), 66.65 (CH_2O from THP), 78.97–79.94 (C alkyne), 97.81 (OCHO). EI MS: 101 (26), 95 (14), 85 (100), 81 (20), 67 (27), 55 (25), 41 (26).

1-Diethyl Phosphonic Ester 18-Tetrahydropyranyloxy-8-undecyne (6). Under an argon atmosphere, a solution of diethyl phosphite (1.7 mL, 13 mmol) in THF (10 mL) was reacted with 300 mg (13 mmol) of sodium. The mixture was refluxed for 1 h until consumption of sodium was complete. Then, 2.71 g of **5** (6.5 mmol) was added and the mixture was refluxed for another 5 h. After evaporation of THF, the product was diluted with CH_2Cl_2 , and the NaBr precipitate was eliminated by filtration on Celite. The solvent was rotary evaporated and the resulting oil was purified by column chromatography on silica gel (eluent $\text{CH}_2\text{Cl}_2/\text{CH}_3\text{OH}$ 98/2) to give 2.55 g of **6** in 83% yield. $^1\text{H NMR}$ (CDCl_3 , ppm): 1.26–1.75 (m, 38H, CH_2 chain, CH_2 from THP, $\text{CH}_3\text{CH}_2\text{OP}(\text{O})$ and $\text{CH}_2\text{P}(\text{O})$), 2.11 (t, 4H, $^3J_{\text{H-H}} = 6.3$ Hz, CH_2 alkyne), 3.36 (m, 2H, CH_2O from THP), 3.71 (m, 2H, CH_2O –THP), 4.07 (q, 4H, $^3J_{\text{H-H}} = 7$ Hz, $\text{CH}_2\text{OP}(\text{O})$), 4.55 (s, br, 1H, OCHO). $^{13}\text{C NMR}$ (CDCl_3 , ppm): 15.38–29.76 (CH_2), 60.31 (d, $^2J_{\text{C-P}} = 6.4$ Hz, $\text{CH}_2\text{OP}(\text{O})$), 61.26 (CH_2O –THP), 66.62 (CH_2O from THP), 78.98–79.25 (C alkyne), 97.79 (OCHO). ^{31}P (CDCl_3 , ppm): 32.50 (s, 1P). EI MS: $m/z = 402$ (18, (THP)), 221 (37), 165 (91), 152 (100), 85 (42), 81 (52), 67 (56), 55 (70), 41 (57).

1-Diethyl Phosphonic Ester 18-Tetrahydropyranyloxyoctadecane (7). The hydrogenation of **6** (1.37 g; 2.65 mmol) was carried out at room temperature in 15 mL of ethanol in the presence of 85 mg of Pd/C catalyst under hydrogen at atmospheric pressure. After 8 h, the catalyst was filtered off using Celite and the filtrate was evaporated to dryness to give 1.31 g (2.65 mmol) of **7**, an oil, in 95% yield. This compound was used in the next step with no further purification. $^1\text{H NMR}$ (CDCl_3 , ppm): 1.24 (s, br, 36H, CH_2 chain and CH_2 from THP), 1.31 (t, 6H, $^3J_{\text{H-H}} = 6.6$ Hz, $\text{CH}_3\text{CH}_2\text{OP}(\text{O})$), 1.61 (m, 2H, $\text{CH}_2\text{P}(\text{O})$), 1.77 (m, 2H, $\text{CH}_2\text{CH}_2\text{O}$ –THP), 3.42 (m, 2H, CH_2O from THP), 3.74 (m, 2H, CH_2O –THP), 4.07 (q, 4H, $^3J_{\text{H-H}} = ^3J_{\text{H-P}} = 6.6$ Hz, $\text{CH}_2\text{OP}(\text{O})$), 4.56 (s, br, 1H, OCHO). $^{13}\text{C NMR}$ (CDCl_3 , ppm): 15.48–29.87 (CH_2), 60.44 (d, $^2J_{\text{C-P}} = 6.4$ Hz, $\text{CH}_2\text{OP}(\text{O})$), 61.40 (CH_2O –THP), 66.77 (CH_2O from THP), 97.91 (OCHO). ^{31}P (CDCl_3 , ppm): 32.64 (s, 1P). EI MS: $m/z = 491$ (1), 376 (42), 165 (42), 152 (100), 85 (43), 55 (23), 41 (22).

1-Diethyl Phosphonic Ester 18-Hydroxyoctadecane (8). A 1.3 g sample of the protected alcohol **7**, (2.65 mmol) was refluxed in 20 mL of ethanol and 1 mL of concentrated HCl for 5 h with stirring. The acidic solution was neutralized with a saturated aqueous NaCO_3 solution until basic, then the mixture was extracted with CH_2Cl_2 . The organic layers were combined and dried over MgSO_4 . The solvent was removed and the crude solid was purified by column chromatography using silica gel to yield 0.88 g of deprotected alcohol **8** (81% yield) as a white solid. Mp = 52 – 53°C . $^1\text{H NMR}$ (CDCl_3 , ppm): 1.24 (s, br, 30H, CH_2 chain), 1.31 (t, 6H, $^3J_{\text{H-H}} = 7$ Hz, $\text{CH}_3\text{CH}_2\text{OP}(\text{O})$), 1.62 (m, 4H, $\text{CH}_2\text{CH}_2\text{OH}$ and $\text{CH}_2\text{P}(\text{O})$), 3.62 (t, 2H,

$^3J_{\text{H-H}} = 6.3$ Hz, CH_2OH), 4.07 (q, 4H, $^3J_{\text{H-H}} = ^3J_{\text{H-P}} = 7$ Hz, $\text{CH}_2\text{OP}(\text{O})$). $^{13}\text{C NMR}$ (CDCl_3 , ppm): 15.48–31.91 (CH_2), 60.44 (d, $^2J_{\text{C-P}} = 6.5$ Hz, $\text{CH}_2\text{OP}(\text{O})$), 62.07 (CH_2O). ^{31}P (CDCl_3 , ppm): 32.75 (s large, 1P). EI MS: $m/z = 407$ (1), 165 (33), 152 (86), 125 (46), 69 (53), 55 (100), 43 (57), 41 (71), 29 (37), 28 (39).

General Procedure for Palladium Insertion in Porphyrin. A 0.308 mmol portion of free base porphyrin and 350 mg of $(\text{C}_6\text{H}_5\text{-CN})_2\text{PdCl}_2$ (0.9 mmol, 3 equiv) were refluxed in 10 mL of benzonitrile under an argon atmosphere for 8 h. Then, 30 mL of methanol was added to the reaction mixture, it was stored in the freezer overnight, and the pink precipitate was filtered off and purified by column chromatography on silica gel (eluent, hexane/ethyl acetate 95/5) to give the pure palladium porphyrin as a pink powder.

Palladium Tetrakis(pentafluorophenyl)porphyrin (12). Eluent: hexane/ethyl acetate 95/5. Yield: 85%. Mp > 250°C dec. $^1\text{H NMR}$ (CDCl_3 , ppm): 8.88 (s, 8H, CH pyrrole). ^{19}F (CDCl_3 , ppm): -136.93 (d, 8F, $^3J_{\text{F-F}} = 21.8$ Hz, F_{ortho}), -151.80 (t, 4F, $^3J_{\text{F-F}} = 21.8$ Hz, F_{para}), -161.73 (t, 8F, $^3J_{\text{F-F}} = 21.8$ Hz, F_{meta}). UV–visible (CH_2Cl_2) λ_{max} (nm): 406 (Soret), 519, 552.

Palladium 5,10,15-Tris(2,6-dichlorophenyl)-20-(pentafluorophenyl)porphyrin (13). Eluent: hexane/ethyl acetate 90/10. Yield: 83%. Mp > 250°C dec. $^1\text{H NMR}$ (CDCl_3 , ppm): 7.74 (m, 9H, CH aromatic), 8.65 (s, 4H, CH pyrrole), 8.72 (s, 4H, CH pyrrole). ^{19}F (CDCl_3 , ppm): -136.76 (d, 2F, $^3J_{\text{F-F}} = 21.8$ Hz, F_{ortho}), -153.00 (t, 1F, $^3J_{\text{F-F}} = 21.8$ Hz, F_{para}), -162.64 (d, 2F, $^3J_{\text{F-F}} = 21.8$ Hz, F_{meta}). UV–visible (CH_2Cl_2) λ_{max} (nm): 411.5 (Soret), 523.5, 557.

General Procedure To Tether the Alkyl Chain on the Porphyrin. Under an argon atmosphere, 5 mL of DMF, the alcohol **7** (1 mmol; 1.5 equiv/aryl group to substitute) and NaH (1 mmol; 1 equiv/alcohol) were stirred at room temperature for 20 min. A solution of palladium porphyrin in DMF (roughly 5 mL for 0.167 mmol of PdP) was then added to the alkoxide. After 1 h, the DMF was removed under vacuum, and the crude solid was purified by silica gel column chromatography.

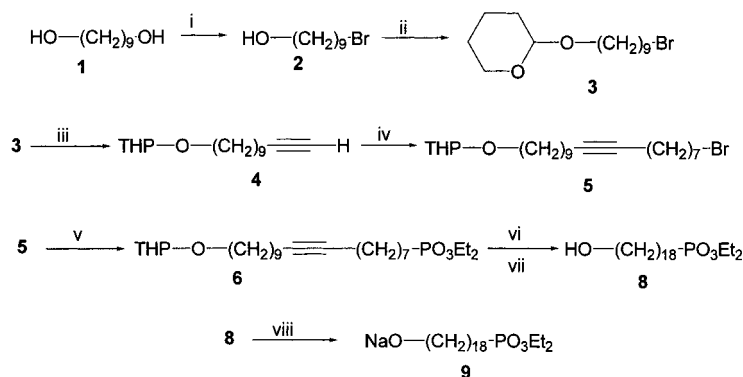
Palladium 5,10,15,20-Tetrakis(diethyl tetrafluorophenyl-4-octadecyloxyphosphonate)porphyrin (14). Eluent: CH_2Cl_2 with increasing methanol quantity until 6%. Yield: 82% as a pink, waxy solid. $^1\text{H NMR}$ (CDCl_3 , ppm): 1.24 (s, br, 120H, CH_2 chain), 1.28 (t, 24H, $^3J_{\text{H-H}} = 7$ Hz, $\text{CH}_3\text{CH}_2\text{OP}(\text{O})$), 1.67 (m, 8H, $\text{CH}_2\text{P}(\text{O})$), 1.99 (m, 8H, $\text{CH}_2\text{CH}_2\text{O}$), 4.05 (q, 16H, $^3J_{\text{H-H}} = 7$ Hz, $\text{CH}_2\text{OP}(\text{O})$), 4.56 (t, 8H, $^3J_{\text{H-H}} = 6.4$ Hz, CH_2O), 8.56 (s, 8H, CH pyrrole). ^{19}F (CDCl_3 , ppm): -139.40 (dd, 8F, $^3J_{\text{F-F}} = 21.8$ Hz, F_{ortho}), -157.78 (dd, 8F, $^3J_{\text{F-F}} = 21.8$ Hz, F_{meta}). ^{31}P (CDCl_3 , ppm): 31.86 (s, 4P). UV–visible: (CH_2Cl_2) λ_{max} (nm): 409 (Soret), 519.5, 552.5. FAB-MS: $m/z = 2625$ (M^+).

Palladium 5,10,15-Tris(2,6-chlorophenyl)-20-(diethyl tetrafluorophenyl-4-octadecyloxyphosphonate)porphyrin (15). Eluent: CH_2Cl_2 with increasing methanol quantity until 2%. Yield: 88%. Mp > 250°C dec. $^1\text{H NMR}$ (CDCl_3 , ppm): 1.30 (s, br, 30H, CH_2 chain), 1.33 (t, 6H, $^3J_{\text{H-H}} = 7$ Hz, $\text{CH}_3\text{CH}_2\text{OP}(\text{O})$), 1.67 (m, 2H, $\text{CH}_2\text{P}(\text{O})$), 2.06 (q, 2H, $^3J_{\text{H-H}} = 6.6$ Hz, $\text{CH}_2\text{CH}_2\text{O}$), 4.1 (q, 4H, $^3J_{\text{H-H}} = ^3J_{\text{H-P}} = 7$ Hz, $\text{CH}_2\text{OP}(\text{O})$), 4.58 (t, 2H, $^3J_{\text{H-H}} = 6.6$ Hz, CH_2O), 7.69–7.83 (m, 9H, CH aromatic), 8.70 (s, 4H, CH pyrrole), 8.75 (d, 2H, $^3J_{\text{H-H}} = 5$ Hz, CH pyrrole), 8.85 (d, 2H, $^3J_{\text{H-H}} = 5$ Hz, CH pyrrole). ^{19}F (CDCl_3 , ppm): -139.21 (dd, 2F, $^3J_{\text{F-F}} = 22.8$ Hz, F_{ortho}), -158.19 (dd, 2F, $^3J_{\text{F-F}} = 22.8$ Hz, F_{meta}). ^{31}P (CDCl_3 , ppm): 32.62 (s, 1P). UV–visible (CH_2Cl_2) λ_{max} (nm): 412.5 (Soret), 523, 556. FAB-MS: $m/z = 1401$ (M^+).

Hydrolysis of the Phosphonic Ester Groups. Under an argon atmosphere, a solution of palladium porphyrin in dry CH_2Cl_2 with Me_3SiBr (20 equiv/ PO_3Et_2 group) was stirred at room temperature for 24 h. The reaction mixture was evaporated and methanol was added to the crude pink solid, the mixture was stirred at room temperature for 3 h, and the solvent was evaporated to give the phosphonic acid. This material was purified on Sephadex G-10 eluted with $\text{CH}_2\text{Cl}_2/\text{CH}_3\text{OH}$ 8/2.

Palladium 5,10,15,20-Tetrakis(tetrafluorophenyl-4-octadecyloxyphosphonic acid)porphyrin (16). Yield was 92% as a waxy solid. $^1\text{H NMR}$ ($\text{CDCl}_3/\text{CF}_3\text{COOD}$ 8/2, ppm): 1.24–1.66 (m, br, 128H, CH_2 chain and $\text{CH}_2\text{P}(\text{O})$), 2.02 (m, 8H, $\text{CH}_2\text{CH}_2\text{O}$), 4.60 (t, 8H, $^3J_{\text{H-H}} = 6.6$ Hz, CH_2O), 8.89 (s, 8H, CH pyrrole). ^{19}F

Scheme 2. Preparation of Precursor 9



i) HBr/bz; ii) DHP, APTS/ether 82%; iii) LiC≡CH, DMSO 82%; iv) nBuLi/THF, Br₂C₇H₁₄-HMPA 86%; v) NaPO₃Et₂/THF 83%; vi) H₂ Pd/C EtOH 95%; vii) HCl/EtOH 81%; viii) DMF, NaH

(CDCl₃/CF₃COOD 8/2, ppm): 140.15 (d, 8F, ³J_{F-F} = 20.3 Hz, F_{ortho}), -158.17 (d, 8F, ³J_{F-F} = 20.3 Hz, F_{meta}). ³¹P (CDCl₃/CF₃COOD (8/2), ppm): 31.20 (s, 4P).

Palladium 5,10,15-Tris(2',6'-chlorophenyl)-20-(tetrafluorophenyl-4'-octadecyloxyphosphonic acid)porphyrin (17). Yield was 96% as a pink solid. Mp > 250 °C dec. ¹H NMR (CDCl₃, ppm): 1.1–2.6 (m, br, 34H, CH₂ chain and CH₂P(O)), 4.54 (t, 2H, ³J_{H-H} = 6.4 Hz, CH₂O), 8.89 (s, 8H, CH pyrrole), 7.54–7.78 (m, 9H, CH aromatic), 8.61–8.71 (m, 6H), 8.83 (d, 2H, ³J_{H-H} = 5 Hz, CH pyrrole). ¹⁹F (CDCl₃, ppm): -139.23 (dd, 2F, ³J_{F-F} = 23.86 Hz and ³J_{F-F} = 5.9 Hz, F_{ortho}), -158.19 (dd, 2F, ³J_{F-F} = 23.6 Hz, and ³J_{F-F} = 8.8 Hz, F_{meta}). ³¹P (CDCl₃, ppm): 30.31 (s, 4P). FAB-MS: m/z = 1345 (M⁺).

Films and Solutions. *Materials.* Octadecylphosphonic acid was used as purchased from Alfa Aesar (Ward Hill, MA). Zirconyl chloride (98%) and octadecyltrichlorosilane (OTS, 95%) were used as supplied from Aldrich (Milwaukee, WI). Amylene-stabilized HPLC grade chloroform was used as received from Acros (Pittsburgh, PA).

Substrate Preparation. Glass microscope slides were purchased from Fischer (Pittsburgh, PA) and were used as substrates for UV-vis and X-ray diffraction studies. The glass substrates were cleaned using the RCA procedure³⁶ and then sonicated for 15 min each in methanol, 50/50 by volume methanol/chloroform, and chloroform. The substrates were then sonicated in a 2% OTS solution in hexadecane and chloroform for 2 h. Finally, the substrates were sonicated for 15 min each in chloroform, 50/50 by volume methanol/chloroform, and methanol.³⁷

Methods. KSV 2000 and KSV 5000 systems (Stratford, CT) were used in combination with homemade, double barrier Teflon troughs for the Langmuir monolayer studies and LB film preparation. The surface areas of the 2000 and 5000 troughs were 343 cm² (36.5 cm × 9.4 cm) and 774 cm² (60.5 cm × 12.8 cm), respectively. A platinum Wilhelmy plate, suspended from a KSV microbalance, measured the surface pressure. Subphases were pure water with a resistivity of 17–18 MΩ cm⁻¹ produced from a Barnstead NANOpure (Boston, MA) purification system.

Zirconium phosphonate LB films were prepared using a three-step deposition technique (Scheme 1).^{23,24} A glass sample vial was placed in the subphase in the well of the trough. The amphiphiles were spread from 0.3 mg mL⁻¹ CHCl₃ solutions and compressed at 15 mm min⁻¹ on the water surface. At the desired pressure, the substrate was dipped down through the monolayer surface and into the sample vial at 8 mm min⁻¹ for OPA and 5 mm min⁻¹ for porphyrin films, transferring the template layer. The substrate and the vial were then removed from the trough and an amount of zirconyl chloride was added to the vial to make the solution ca. 4 × 10⁻⁵ M in Zr⁴⁺. After 20 min in the zirconium solution, the substrate was removed from the vial and rinsed with water. To form the capping layer

and complete the bilayer, the now hydrophilic substrate was lowered into the trough, a monolayer was spread and compressed to the desired pressure, and the substrate was raised through the monolayer surface at 5 mm min⁻¹ for OPA and 3 mm min⁻¹ for porphyrin monolayers.

The creep of the pure porphyrin Langmuir monolayers was studied at high and low pressures over 30 min, or roughly the time of one deposition. At a constant high pressure (12–15 mN m⁻¹), the area changed by 6% and 12% for **16** and **17**, respectively. At low pressure (3–5 mN m⁻¹), the change in area was 3% and 7% for **16** and **17**, respectively. The instability in the monolayers led to a necessary correction in the transfer ratios. The corrected transfer ratios for the pure **16** were 1.0–1.4 at high pressures and 1.0–1.1 at low pressures. For the pure **17**, the corrected transfer ratios were 0.8–1.0 and 0.9–1.0 for high pressure and low pressure transfers, respectively. The transfer ratios of the porphyrin films mixed with OPA consistently showed uncorrected transfer ratios near unity.

Transmittance UV-visible experiments were performed on a Hewlett-Packard series 8452A diode array spectrophotometer and a Cary 50 spectrophotometer by Varian. Both instruments had an average resolution of 2 nm. A plane, visible polarizer was used to select s- and p-polarized light. A Teflon sample holder with grooves cut at 45° to one another was used to obtain sampling at 0° (beam normal to the substrate) and 45° incidence to the substrate surface. Reflectance UV-vis experiments were performed on a KSV 2000 minitrough using an Oriel spectrophotometer and a 77410 filter with a range from 200 to 600 nm. X-ray diffraction patterns were obtained with a Phillips APD 3720 X-ray powder diffractometer with the Cu Kα line, λ = 1.54 Å, as the source.

Results

Synthesis. The key reaction for the preparation of the organic precursors was the aromatic nucleophilic substitution; consequently, the needed precursors were the porphyrins **12** and **13** and the alcohol **8** (Schemes 2 and 3). Porphyrins **10** and **11** were synthesized as described previously^{34,35} and metalated according to the classical procedure using Pd (PhCN)₂Cl₂ in refluxing benzonitrile.³⁸ The preparation of molecule **8** was inspired by a synthetic route developed for α,ω-disubstituted alkyl chains and is presented in Scheme 2.³⁹

First, 1,9-nonanediol **1** was monobrominated using HBr in benzene.³³ The alcohol group was protected with a THP ether⁴⁰ and was treated with lithium acetylide—

(38) Buchler, J. *Porphyrins and Metalloporphyrins*; Smith Elsevier Scientific Publishing Company: 1975.

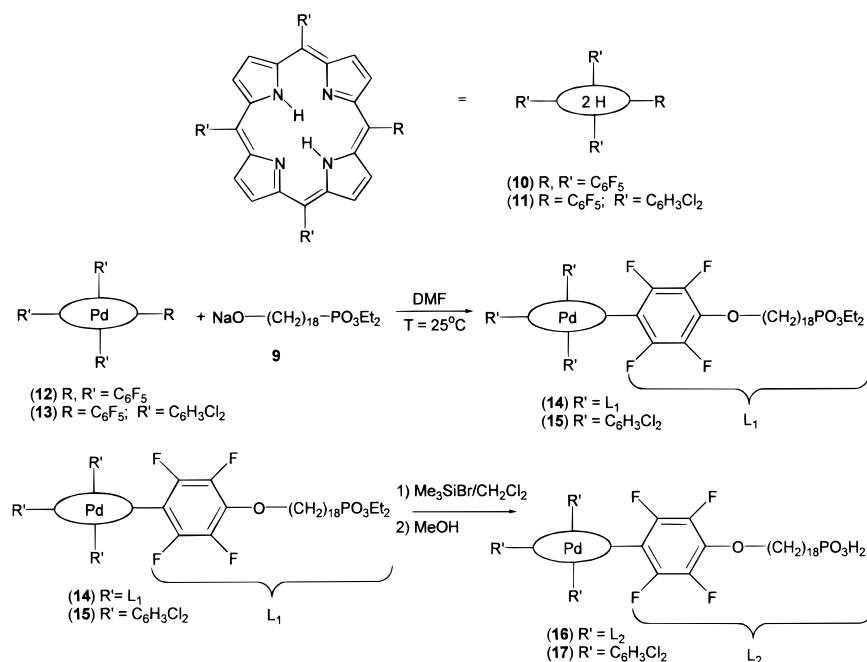
(39) Naoshima, Y.; Nakamura, A.; Munakata, Y.; Kamezawa, M.; Tachibana, H. *Bull. Chem. Soc. Jpn.* **1990**, *63*, 1263–1265.

(40) Reese, C. *Protective Groups in Organic Chemistry*; Plenum Press: London, 1973.

(36) Kern, W. *J. Electrochem. Soc.* **1990**, *137*, 1887–1892.

(37) Advincula, R. Ph.D. Thesis, University of Florida, 1994.

Scheme 3. Preparation of 16 and 17



ethylenediamine to give the terminal alkyne **4** in 82% yield.⁴¹ The alkyne **4** was alkylated with an excess of 1,7-dibromoheptane after deprotonation with ^tBuLi to give the bromo-protected alcohol **5** in 83% yield from **4**. The phosphonic ester was introduced via a Michaelis–Becker reaction by treatment of the bromo compound **5** with the sodium salt of diethyl phosphite. The triple bond of **6** was reduced by hydrogen on Pd/C, and the THP protecting group was removed with HCl in refluxing ethanol, leading to the desired 1-diethyl phosphonic ester 18-hydroxyoctadecane **8** (Scheme 2).

Functionalization of the porphyrin was successfully achieved in DMF at room temperature by reacting the alkoxide derived from **8** and NaH with the metalated porphyrins **12** or **13** (Scheme 3). Finally, the phosphonic ester group was smoothly hydrolyzed in quantitative yield with Me₃SiBr following the mild procedure developed by McKenna.⁴²

Solutions. The palladium porphyrins show spectral responses in the UV–vis consistent with hypo-type metalloporphyrins. For each porphyrin, a strong Soret band (or B band) is present above 400 nm and two Q bands are centered around 550 nm.^{43,44} The Soret band is associated with an allowed transition between the singlet ground state (a₁ or S₀) and a high energy singlet excited state (e_g or S₂).^{43,44} This band is very sensitive to the porphyrin environment, including interchromophore interactions.¹⁹

Three types of aggregation of porphyrin chromophores have been observed, and the Soret band can be used to identify the modes of interaction.¹⁹ In face-to-face or H-type aggregates, the Soret shifts to the blue relative to the nonaggregated porphyrins. Porphyrins can also

aggregate in an edge-to-edge arrangement, in which case the spectral components of the Soret band splits and part of the band shifts red and part shifts blue. Finally, the chromophores can form head-to-tail or J aggregates, which cause a red shift in the Soret band.

Solution studies of the porphyrins **16** and **17** were performed in ethanol and chloroform, and the absorbance dependence on concentration was investigated. Solutions ranging from 10⁻¹² to 10⁻⁶ M were studied. In CHCl₃, the Soret band was consistently at 410–411 nm for the porphyrin **16**. It is apparent that in CHCl₃, **16** shows no sign of solution aggregation. For porphyrin **17** at 10⁻¹² M, the Soret band absorbed at 411 nm; however, as the concentration was raised, the band shifted red to 414 nm. Because **17** has only one long chain substituent, the likelihood of aggregation is increased, and in CHCl₃, the chromophores apparently J aggregate at high concentrations.^{18,19} Interestingly, the Soret bands for both **16** and **17** absorb at 411 nm at 10⁻¹² M, so the long chains have no effect on the Soret of the nonaggregated chromophore.

The studies of the same molecules at identical concentrations in EtOH showed very different behavior. At 10⁻¹² M, both **16** and **17** show Soret bands at 414–415 nm. This peak is significantly to the red of the Soret bands in CHCl₃; however, it is known that more polar solvents tend to stabilize the excited states in π–π* transitions, shifting this band to lower energies.⁴⁵ As the concentrations of both **16** and **17** were raised, the Soret band systematically shifted blue to 407 and 411 nm for the porphyrins **16** and **17**, respectively implying H aggregation of the chromophores in EtOH.^{18,19}

Langmuir Monolayers. The room-temperature pressure vs area isotherm of **16** on water at pH 5.5 is shown in Figure 2a. There is a measurable onset of surface pressure near 220 Å² molecule⁻¹, followed by a gradual increase in pressure as the film is compressed, with an

(41) Smith, W.; Beumel, O. *Synthesis* **1974**, 441–442.

(42) McKenna, C. E.; Higa, M. T.; Cheung, N. H.; McKenna, M.-C. *Tetrahedron Lett.* **1977**, 155–158.

(43) *The Porphyrins*; Dolphin, D., Ed.; Academic Press: New York, San Francisco, London, 1978; Vol. III.

(44) Caughey, W.; Deal, R.; Weiss, C.; Goutermann, M. *Journal of Molecular Spectroscopy* **1965**, *16*, 451–463.

(45) Lambert, J. B.; Shurvell, H. F.; Lightner, D.; Cooks, R. G. *Introduction to Organic Spectroscopy*; Macmillan: New York, 1987.

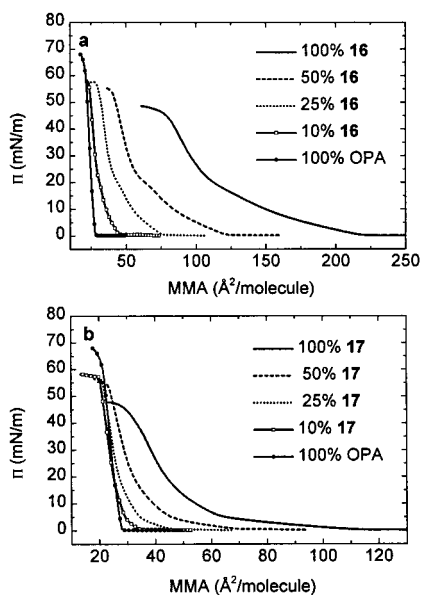


Figure 2. Surface pressure (Π) vs mean molecular area (MMA) isotherms: (a) **16** and (b) **17** as pure films and as mixtures with OPA.

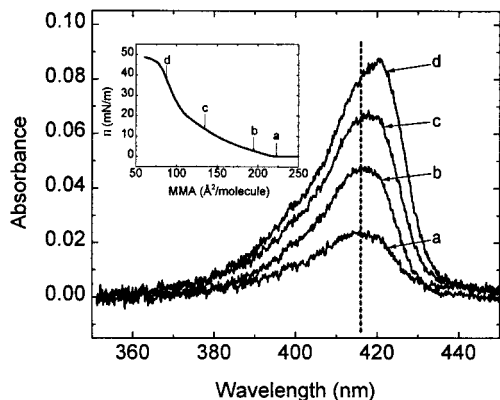


Figure 3. Reflectance UV-vis of **16** on the water surface showing the Soret band as the MMA is decreased. The Soret band of **16** shifts to higher wavelengths with compression, indicating an increase in chromophore aggregation. The spectra were obtained under the corresponding conditions, indicated on the isotherm shown in the inset.

apparent phase transition giving a steeper rise in pressure near $115 \text{ \AA}^2 \text{ molecule}^{-1}$. The MMA of the tetraphenyl porphyrin itself is approximately $200 \text{ \AA}^2 \text{ molecule}^{-1}$, implying that at the onset, the tetrasubstituted porphyrin molecules are not aggregated or stacked.¹⁶ However, this arrangement is not stable to pressure, and as the film is compressed, the molecules are forced to rearrange.

The change in the aggregation of **16** during compression can be observed with reflectance UV-vis spectroscopy of the Langmuir monolayer (Figure 3). As the film is compressed from a MMA of $370 \text{ \AA}^2 \text{ molecule}^{-1}$ through $220 \text{ \AA}^2 \text{ molecule}^{-1}$, the λ_{max} remains between 416 and 417 nm, similar to the λ_{max} seen for the nonaggregated porphyrin in EtOH. At areas between 220 and $100 \text{ \AA}^2 \text{ molecule}^{-1}$, the Soret band shifts to 418–419 nm, and below $100 \text{ \AA}^2 \text{ molecule}^{-1}$ the Soret band shifts further to near 421 nm. The shift in the Soret band suggests a change in the interaction of the chromophores at different pressures. At MMA larger than and comparable to the size of the chromophore

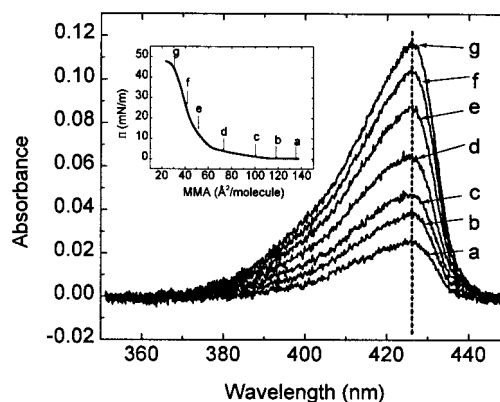


Figure 4. Reflectance UV-vis of **17** on the water surface showing the Soret band as the MMA is decreased. No shift in the Soret band was observed as the monolayer was compressed, implying that the chromophores were already aggregated upon spreading. The spectra were obtained under the corresponding conditions indicated on the isotherm shown in the inset.

itself, the porphyrin rings cannot be aggregating to any significant extent or the onset of surface pressure would occur at lower areas. The red shift of the Soret band as the area is decreased indicates enhanced chromophore aggregation at lower MMA.

In contrast to **16**, the π - A isotherm of **17** (Figure 2b) indicates that this molecule aggregates even in the absence of applied pressure. No significant increase in surface pressure is seen until areas below $120 \text{ \AA}^2 \text{ molecule}^{-1}$. The pressure rises to only 5 mN m^{-1} at $60 \text{ \AA}^2 \text{ molecule}^{-1}$, below which the pressure increases until the film collapses below $36 \text{ \AA}^2 \text{ molecule}^{-1}$. The isotherm cannot reflect a true molecular monolayer, but rather results from the compression of aggregates at the water surface. Evidence of aggregation at all MMA is seen in reflectance UV-vis spectra. Figure 4 shows the Soret band as a function of MMA from greater than $120 \text{ \AA}^2 \text{ molecule}^{-1}$ to film collapse at $36 \text{ \AA}^2 \text{ molecule}^{-1}$. The Soret band does not shift during compression, and the λ_{max} of 426 nm indicates that the porphyrins are aggregated at each stage of the isotherm.

A common procedure for enhancing the stability and processibility of unstable Langmuir monolayers is to mix the amphiphile of interest with a good film-forming amphiphile.^{9,13-15} Each of the porphyrins was mixed with OPA, which is a well-studied amphiphile that forms a liquid-condensed phase on the water surface. As the percentage of OPA is increased, the isotherms increasingly take on characteristics of the liquid-condensed phase of OPA (Figure 4), although features present in the isotherms of the pure porphyrins are also present in the isotherms of the mixed films. In addition, the collapse pressure increases with the concentration of OPA, indicating that the films become more stable as OPA is added. However, diluting the porphyrin film with OPA does not appear to greatly affect the aggregation. Reflectance UV-vis of a Langmuir monolayer of a 1:9 mixture of **16** with OPA is shown in Figure 5. The λ_{max} shifts from 415.5 nm at high MMA to 420 nm as the film is compressed, just as it does in the films of pure **16** (Figure 3). The porphyrins do not appear to be aggregated in the mixed film at high MMA.

The molecular areas in Figures 2 and 5 are weighted averages of the porphyrin and OPA molecules. The

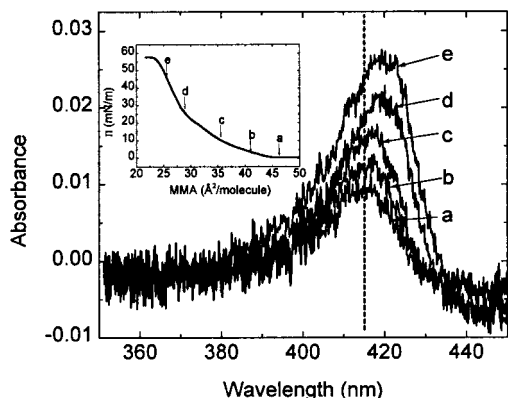


Figure 5. Reflectance UV-vis of 10% **16** (90% OPA) on the water surface showing the Soret band as the MMA is decreased. A Soret band shift similar to the pure porphyrin **16** (Figure 3) is observed as the monolayer is compressed. The spectra were obtained under the corresponding conditions indicated on the isotherm shown in the inset.

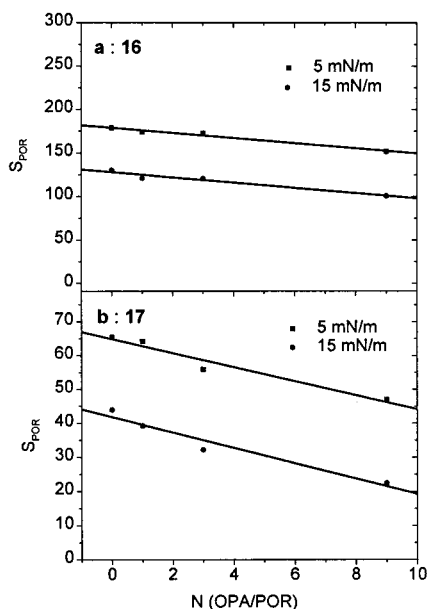


Figure 6. Changes in the area per porphyrin molecule (S_{POR}) at 5 and 15 mN m^{-1} as a function of the ratio of OPA to porphyrin (N) in the Langmuir monolayers of (a) **16** and (b) **17**. Data are obtained from the Π vs MMA isotherms shown in Figure 2.

MMA of the porphyrin molecules in the mixed films can be calculated using eq 1:¹⁴

$$S_{\text{MIX}} = \frac{(S_{\text{POR}} + NS_{\text{OPA}})}{(N + 1)} \quad (1)$$

where S_{MIX} is the MMA of the mixture determined from the isotherm, S_{POR} is the MMA of the porphyrin within the mixed films, S_{OPA} is the MMA of the OPA amphiphile in pure OPA films, and N is the ratio of OPA to porphyrin. S_{POR} was calculated in the OPA mixtures of each porphyrin at pressures of 5 and 15 mN m^{-1} , and the results are plotted in Figure 6. If the OPA diluent were breaking apart the preferred organization of the porphyrins in the films, S_{POR} would increase as the aggregates separate. The decrease in S_{POR} in the mixed films suggests that either the porphyrin chromophores are reorienting in the mixed films or aggregation

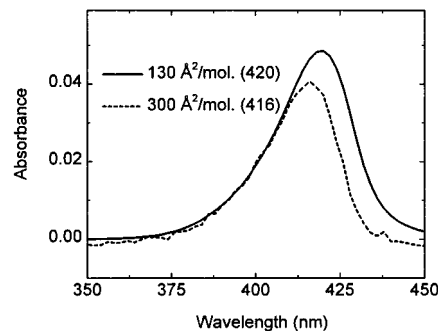


Figure 7. Transmittance UV-vis of **16** in alternating Langmuir-Blodgett films transferred at high and low MMA. The absorbance scale corresponds the spectrum of the film transferred at 300 $\text{\AA}^2 \text{ molecule}^{-1}$. The other spectrum is scaled in intensity for comparison of band shapes and wavelengths. The λ_{max} (nm) of each spectrum is given in parentheses.

actually increases in the mixed films. However, it does not appear that porphyrin aggregation decreases in the mixed monolayers.

Langmuir-Blodgett Films. LB films of **16** and **17** were prepared using the deposition procedure described in Scheme 1. The stepwise deposition allows fabrication of both symmetric films, where the template and capping monolayers are the same, and alternating films, where the two monolayers in the bilayer are different. Both types of films were prepared for each porphyrin (Figure 1). We have previously shown that a zirconated octadecylphosphonic acid template layer frequently provides the best substrate for transferring a capping layer.³⁰ The extremely well-organized and oxophilic surface allows deposition of almost any phosphonic acid monolayer, including those that are not stable monolayers and would normally not transfer. Monolayers of **16** and **17** were transferred at a range of temperatures, pressures, and subphase pHs (Tables 1 and 2). Films of the porphyrins mixed with OPA were also transferred under a variety of conditions. Under some conditions, perfect, organized monolayers were obviously not formed, but the films were still able to be transferred onto solid supports and studied.

Films of Compound 16. To form alternating films of **16**, the Langmuir monolayers were transferred as capping layers onto zirconated OPA template layers. Films were transferred at different points along the π - A isotherm, and the Soret band of the transferred films was used to monitor differences in chromophore aggregation in the deposited films. The UV-vis spectrum of a film transferred at 130 $\text{\AA}^2 \text{ molecule}^{-1}$ (15 mN m^{-1}) is shown in Figure 7, where the λ_{max} of the Soret band appears at 420 nm, significantly red-shifted from any band of the solution spectra of **16**. The red-shift suggests increased aggregation, which is expected because, at such a small MMA, the chromophores must be either tilting perpendicular to the surface and organizing side-by-side or sliding over one another to form bilayers or multilayers. Polarized UV-vis spectroscopy (described below) indicates that the porphyrins are oriented parallel to the surface, implying the latter arrangement.

Layers of **16** were also transferred at 190 $\text{\AA}^2 \text{ molecule}^{-1}$ (12 mN m^{-1}) and at 300 $\text{\AA}^2 \text{ molecule}^{-1}$, before the onset of any surface pressure. The Soret band shifts to 418 nm for the film transferred at 190 $\text{\AA}^2 \text{ molecule}^{-1}$ and to

Table 1. UV–Vis Data from Symmetric and Alternating Films of 16

film	MMA of transfer (Å ² /molec) ^a	Π of transfer (mN/m) ^b	pH ^c	temp (°C)	λ _{max} ^d (nm)	thickness ^e (Å)
OPA/Zr/16	300	-	5.5	23–25	416	
OPA/Zr/16	190	4	5.5	23–25	418	42
OPA/Zr/16	180	5	5.5	23–25	418	
OPA/Zr/16	130	15	5.5	23–25	420	
OPA/Zr/16	100	25	5.5	23–25	420	
OPA/Zr/16	90	35	5.5	23–25	420	
OPA/Zr/10% 16	37	5	5.5	23–25	415	
OPA/Zr/10% 16	35	15	5.5	23–25	418	47
OPA/Zr/25% 16	50	15	5.5	23–25	420	
OPA/Zr/50% 16	74	15	5.5	23–25	420	
OPA/Zr/16	300		9.4	23–25	416	
OPA/Zr/16	190	4	9.4	23–25	416	
OPA/Zr/16	300		11.1	23–25	414	
OPA/Zr/16	85	15	5.5	40	419	
OPA/Zr/16	160	4	5.5	40	417	
OPA/Zr/25% 16	50	15	5.5	40	415	
OPA/Zr/25% 16	60	4	5.5	40	415	
OPA/Zr/10% 16	35	15	5.5	40	415	
OPA/Zr/10% 16	50	4	5.5	40	415	
16/Zr/16	190	4	5.5	23–25	416	
16/Zr/16	130	15	5.5	23–25	418	
10% 16/Zr/10% 16	37	5	5.5	23–25	418	47

^a Area of the chromophore and diluent as determined from Figure 2 (isotherms). ^b Corresponding pressure from Figure 2 (isotherms). ^c pH of nanopure water from filtration system is about 5.5. ^d λ_{max} is given for monolayers. ^e Interlayer thickness is given for multilayers of films transferred under a variety of transfer conditions.

Table 2. UV–Vis Data from Symmetric and Alternating Films of 17

film	MMA of transfer (Å ² /molecule) ^a	Π of transfer (mN/m) ^b	temp (°C)	λ _{max} ^c (nm)	thickness ^d (Å)
OPA/Zr/17	73	4	23–25	424	
OPA/Zr/17	52	12	23–25	426	61
OPA/Zr/17	41	25	23–25	428	
OPA/Zr/17	38	30	23–25	428	
OPA/Zr/17	36	35	23–25	428	
OPA/Zr/10% 17	30	4	23–25	424	
OPA/Zr/10% 17	27	12	23–25	426	48
OPA/Zr/25% 17	30	12	23–25	426	
OPA/Zr/50% 17	38	12	23–25	426	
OPA/Zr/17	73	4	40	424	
OPA/Zr/17	52	12	40	424	
OPA/Zr/10% 17	30	4	40	424	
OPA/Zr/10% 17	27	12	40	424	
OPA/Zr/10% 17	26	20	40	425	
OPA/Zr/25% 17	30	12	40	426	
17/Zr/17	52	12	23–25	426	
10% 17/Zr/10% 17	26	20	23–25	426	48

^a Area of the chromophore and diluent as determined from Figure 2 (isotherms). ^b Corresponding pressure from Figure 2 (isotherms). ^c λ_{max} is given for monolayers, and ^d interlayer thickness is given for multilayers of films transferred under a variety of transfer conditions.

416 nm for the film transferred at 300 Å² molecule⁻¹, indicating less aggregation in these films. At these larger MMA, the porphyrin chromophores should be lying flat at the air–water interface with little aggregation, and they appear to remain noninteracting when transferred.

As the pH is raised, the amphiphiles become slightly soluble and the monolayer becomes increasingly susceptible to creep. However, films of **16** compressed to 300 Å² molecule⁻¹ were deposited onto zirconated OPA templates from subphases of pH 9.4 and 11.1. As the pH increases, λ_{max} of the Soret band of the transferred film decreases until 414 nm for the film deposited at pH 11.1. This is the lowest value of λ_{max} that we have observed for any transferred film of **16**, and we consider it to be characteristic of a nonaggregated assembly. The λ_{max} of this Soret band corresponds to that of chromophore **16** in EtOH at 10⁻¹² M, which we have concluded to be nonaggregated.

The transition moment of the Soret band lies within the plane of the porphyrin macrocycle and polarized UV–vis spectroscopy can be used to determine the orientation of the porphyrin in the transferred films. Experimentally, a dichroic ratio (*D*) is measured:¹³

$$D = \frac{A_s}{A_p} \quad (2)$$

where *A_s* and *A_p* are the absorbances with s-polarized (parallel to the dipping direction) and p-polarized (perpendicular to the dipping direction) light, respectively. If *D* is measured at two incident angles, 0° and 45°, then both the in-plane and out-of-plane orientations of the porphyrin can be determined using the procedure described by Möbius.^{46,47}

Consistently, $D = 1 \pm 0.02$ when measured at 0° incidence, indicating no preferred in-plane orientation of the chromophore. However, in all films, $D \neq 1$ when measured at 45° incidence. For films transferred at high surface area, it is expected that the porphyrins should lie flat with all four phosphonates tethered to the surface. Indeed, this is observed for films transferred at 190 and 300 \AA^2 molecule $^{-1}$ where the tilt angle, θ , with respect to the surface normal is observed to be 90° . Interestingly, the porphyrins also appear to lie parallel to the surface in the films transferred at 130 \AA^2 molecule $^{-1}$, where θ is also measured as approximately 90° . The result implies that in films transferred at areas smaller than the MMA of the flat porphyrin macrocycle, the molecules overlap, stacking in bilayers or multilayers but with very little change in the tilt angle. There is a larger uncertainty, possibly $\pm 10^\circ$, in the measurement as the tilt angles near 90° ,⁴⁶ however, our results confirm that the chromophores are lying approximately flat in all of the films in this study.

Multilayers of the alternating OPA/Zr/**16** films can be deposited, and X-ray diffraction confirms the layered nature of the films. Two or three orders of the (00 l) Bragg peaks can be observed in each case. Films transferred at 190 \AA^2 molecule $^{-1}$ have a bilayer thickness of 42 \AA , which is smaller than the 48 \AA thickness seen in pure OPA/Zr/OPA bilayers,²³ suggesting that the 18-carbon tethers of **16** are not fully extended in the alternating films. For the film transferred at 130 \AA^2 molecule $^{-1}$, the bilayer thickness increases to 47 \AA as the tetrasubstituted chromophores begin to overlap.

Symmetric bilayers of **16**/Zr/**16**, fabricated according to Scheme 1, were also studied. Porphyrin **16** could be transferred on the down stroke under a variety of conditions. After zirconation, deposition of a capping layer of **16** results in a symmetric bilayer. The Soret band is very similar to that from alternating films deposited at the same area per molecule, and polarized UV-vis indicates that the porphyrins are also lying parallel to the surface. However, the layers are poorly organized, as (00 l) Bragg peaks could not be seen in diffraction from 9-bilayer films. It is probably poor organization in the template layer of porphyrin **16** that is responsible for the lack of a well-defined layered structure.²⁴

Mixed monolayers of **16** with OPA were transferred onto OPA templates at different points along the surface pressure vs area isotherms, as shown in Table 1, and the aggregation of the porphyrin in the transferred film parallels that seen in the films of the pure porphyrins. For films transferred at pressures of 15 mN m^{-1} , the Soret band appears at 420 nm, shifting to 415 nm when transferred at pressures less than 5 mN m^{-1} , which, again, corresponds to the nonaggregated form seen in EtOH. In all cases, polarized UV-vis indicates that the porphyrins orient parallel to the surface.

The mixed monolayers show an interesting effect with increased temperature. A mixed monolayer of 10% **16** with OPA transferred at 15 mN m^{-1} on a subphase heated to 40 $^\circ\text{C}$ shows a Soret band λ_{max} of 415 nm, shifted from 420 nm for the same film deposited at room

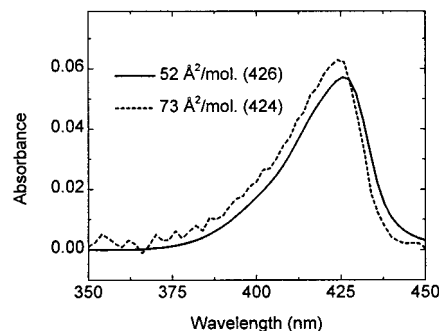


Figure 8. Transmittance UV-vis of **17** in alternating Langmuir-Blodgett films transferred at high and low MMA. The absorbance scale corresponds to the spectrum of the film transferred at 73 \AA^2 molecule $^{-1}$. The other spectrum is scaled in intensity for comparison of band shapes and wavelengths. The λ_{max} (nm) of each spectrum is given in parentheses.

temperature. As the subphase is heated, the aggregates appear to break up in the mixed film. A similar effect is not seen on the pure films of **16**. It appears that the OPA plays a role in breaking up the aggregates at higher temperatures.

Films of Compound 17. The π -A isotherms and the reflectance UV-vis experiments described above indicate that the molecules of **17** aggregate upon spreading, and this aggregation is preserved in the transferred films. In contrast to **16**, the monophosphonate **17** is only slightly influenced by attempts to break up the aggregates by changing the deposition conditions. The UV-vis spectrum of a capping layer of **17** transferred at 52 \AA^2 molecule $^{-1}$ (12 mN m^{-1}) is shown in Figure 8, where the Soret band appears at 426 nm, consistent with the value observed in the reflectance spectrum taken from the water interface. The shape of the Soret band does not change for films deposited at higher MMA, higher temperatures, or in mixtures with OPA, and the position shifts only slightly (Table 2). The orientation of the chromophores was also unaffected by the deposition conditions. Polarized spectra consistently give tilt angles of 90° , corresponding to the porphyrins lying flat.

X-ray diffraction from a film of **17** transferred at 52 \AA^2 molecule $^{-1}$ onto a zirconated OPA template gives a layer thickness of 61 \AA (Table 2). This thickness is larger than that of the alternating films of OPA/Zr/**16** or OPA/Zr/OPA bilayers.²³ Since optical spectroscopy indicates that the molecules lie flat, the enhanced thickness of the layer suggests that they transfer as stacked bilayers or multilayers. Further evidence for this arrangement comes from the film stability studies, described below, which indicate that part of the transferred film of porphyrin **17** is physisorbed to the surface.

Film Stability. Zirconium phosphonate LB films are insoluble in organic solvents due to the cross-linking within the zirconium-phosphonate extended network.²³ To monitor how well the porphyrin layers bind to the zirconated template, transferred films of **16** and **17** were rinsed with chloroform in a Soxhlet extractor. Figure 9 shows the absorbances at λ_{max} of the Soret band as a function of washing time in the Soxhlet extractor. Figure 9 shows that none of the film of **16** is washed away after 1 h in chloroform, suggesting that all of the molecules are tethered to the zirconated OPA template. The same

(47) Mobius, D.; Orrit, M.; H., G.; Meyer, H. *Thin Solid Films* **1985**, *132*, 41-53.

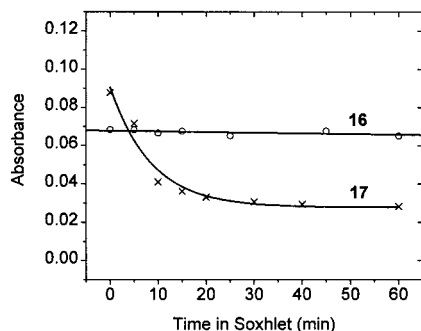


Figure 9. Absorbance of OPA/Zr/porphyrin bilayers as a function of time the films were exposed to chloroform in a Soxhlet extractor. The film of **16** was transferred at 15 mN m⁻¹ and room temperature and the film of **17** was transferred at 12 mN m⁻¹ and room temperature.

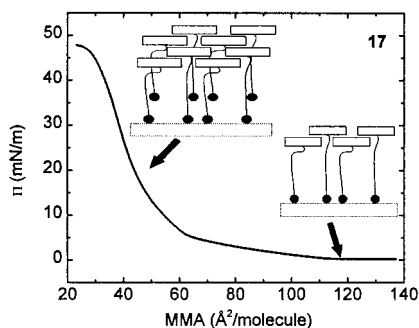


Figure 10. Schematic illustrating the possible packing of amphiphiles **17** in transferred films when deposited at high and low MMA. The white rectangles represent the chromophores, the black lines represent the alkyl chains, and the black circles represent the phosphonate headgroups. At both high and low MMA, the chromophores are aggregated, but as the film is compressed, the aggregates start stacking, making it impossible for some of the phosphonates to bind to the zirconium layer in the transferred films. These physisorbed chromophores are then easily removed by hot chloroform.

result was obtained for films of **16** deposited at both higher and lower pressures or in mixtures with OPA.

In contrast, the absorbance of the LB films of **17** exposed to CHCl₃ decreased significantly, due to the desorption of chromophores. The absorbance leveled off after 20 min, to a value corresponding to the truly surface confined chromophores (Figure 9). This result suggests that the stacked layers of chromophores in the porphyrin **17** films were partially physisorbed on the surface.

Discussion

The behavior of the monosubstituted and tetrasubstituted porphyrins is very different on the water surface, and the differences are carried over to the transferred films. Porphyrin **17** spreads on the water surface to a limited extent. Our proposal for how the molecules behave on the water surface is shown schematically in Figure 10. Optical spectroscopy indicates that **17** aggregates, but the π - A isotherm and X-ray diffraction from the transferred layers suggest that the aggregates are only a few molecules thick. The aggregates are present at both high and low MMA and can be transferred, as aggregates, onto the zirconated OPA templates. Some molecules from each aggregate chemisorb to the zirconated surface through zirconium

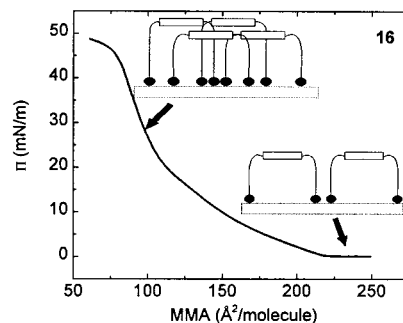


Figure 11. Schematic illustrating the possible packing of amphiphiles **16** in transferred films when deposited at high and low MMA. The white rectangles represent the chromophores, the black lines represent the alkyl chains, and the black circles represent the phosphonate headgroups. At high MMA, the alkyl chains are disordered and the chromophores are not aggregated. At low MMA, the alkyl chains are still disordered; however, the chromophores are forced to aggregate.

phosphonate linkages, but some are physisorbed as part of the preformed aggregates. When exposed to hot chloroform, the physisorbed part of the film is dissolved away.

Chemical modification with four alkylphosphonic acid side groups allows the porphyrin to spread completely. Porphyrin **16** spreads to a monolayer thick film at high MMA, and as the film is compressed, an increase in surface pressure is registered near 200 Å² molecule⁻¹, corresponding to the area of the flat porphyrin macrocycle. However, the side-by-side arrangement of the porphyrin chromophores is not stable, as the pressure is increased and the film rearranges, with the molecules either standing on edge or sliding over one another to form multiple layers. This behavior is illustrated in Figure 11.

The films of **16** can be transferred at high MMA onto zirconated OPA templates to form monolayer or sub-monolayer films of the porphyrin chemisorbed to the surface with the chromophore ring oriented parallel to the surface. Films of **16** can also be transferred at lower MMA, where the reflectance UV-vis indicates that the porphyrins are interacting. Analysis of the transferred films suggests that the porphyrin chromophores are lying flat, overlapping each other to form layers that are a few molecules thick. In contrast to the films of **17**, all of the molecules in the aggregated films of **16** appear to be chemisorbed to the surface. None of the film is lost during rinsing with hot chloroform. The different behavior probably results from the fact that four phosphonic acid groups increase the chance of each molecule bonding onto the zirconium phosphonate network. Any orientation of the porphyrin macrocycle will direct at least one alkylphosphonic acid side chain toward the surface.

Whether the Langmuir monolayers are transferred intact or reorganize during film transfer is not yet clear. At high MMA, molecules of **16** lie flat on the water surface, and this arrangement seems to be preserved in the transferred films. However, when the films are transferred at lower MMA, where the films are clearly aggregated, there could be some rearrangement. There is a significant driving force for forming zirconium phosphonate linkages, and the aggregates could rearrange during transfer to maximize interactions with the

zirconated surface. While the porphyrins are clearly oriented parallel to the surface in the transferred film, providing each porphyrin the chance to form multiple zirconium phosphonate bonds, it is not known if the molecules aggregate the same way on the water surface.

The LB procedure used in these studies takes advantage of the binding energy of the zirconium phosphonate continuous lattice and is shown to be quite versatile. Both symmetric and alternating layer films can be prepared. Use of the zirconated OPA template layer allows almost any phosphonic acid derivatized amphiphile to transfer in a capping layer.^{23,24,27,30} Unlike conventional LB depositions, films of **16** and **17** can be transferred onto the zirconated template layers at any surface pressure, allowing, in the case of **16**, the arrangement of the molecules in the transferred films to be tuned by choice of the area-per-molecule at deposition. The films do not need to be stable Langmuir monolayers in order to transfer, as the driving force is formation of the zirconium–phosphonate bonds. It is the strength of the zirconium–phosphonate interaction, in particular the lattice energy associated with the zirconium phosphonate extended network, that is responsible for the exceptional stability of these LB films.^{23,24} Zirconium phosphonate LB films, like solid-state zirconium phosphonates, are insoluble in organic solvents and under most aqueous conditions. The inorganic network has also been shown to enhance the thermal stability of LB films.⁴⁸

Conclusion

LB films of the amphiphiles **16** and **17** were prepared that incorporate a zirconium phosphonate inorganic extended solid network into the hydrophilic region of the films. Symmetric films, where both layers of the bilayer contain the porphyrin, and alternating films,

where the template layer is OPA and the capping layer contains the porphyrin, were prepared. The zirconium phosphonate deposition procedure allows transfer of the porphyrin films under a variety of conditions, providing a means for controlling the degree of porphyrin aggregation in the transferred films.

Very different results were observed for the mono- and tetrasubstituted porphyrins. The monophosphonic acid **17** aggregates on the LB trough, and this aggregation remains in the transferred films. On the other hand, the tetraphosphonic acid **16** spreads to a monolayer on the water surface and the degree of aggregation can be altered in transferred films by varying the deposition conditions. Films of **16** deposited at high MMA are comprised of weakly interacting chromophores oriented parallel to the surface.

The zirconium phosphonate inorganic extended network adds substantial stability to the films, which are insoluble under most organic and aqueous conditions. The methods developed here with the palladium tetraphenylporphyrins can also be applied to other porphyrin systems, and in this way the vast array of physical and chemical characteristics of porphyrins, including catalytic activity, should be able to be incorporated in stable LB films.

Acknowledgment. We would like to thank the National Science Foundation (D.R.T.) and CNRS (B.B. and F.O.) for financial support. We thank Dr. Kirk Schanze for use of the HP spectrophotometer, Dr. Randy Duran and Jennifer Batten for use of and assistance with the Oriel spectrophotometer, and Daniel Maume in Ecole Vétérinaire de Nantes for recording FAB mass spectra. We would also like to thank the University of Florida Major Analytical Instrumentation Center for use of the XRD facilities.

(48) Petruska, M.; Talham, D. Unpublished results.